GLOBAL JOURNAL OF PURE AND APPLIED SCIENCES VOL. 12, NO. 3, 2006: 387 - 395

APPLICATION OF GEOPHYSICAL WIRELINE LOGS IN HYDROCARBON RESERVIOR CHARACTERIZATION: A CASE STUDY FROM ONSHORE NIGER DELTA

M. A. AYUK, M. T. OLOWOKERE, and E. A. ARIYIBI

(Received 4 July, 2005; Revision Accepted 12 September, 2005)

ABSTRACT

A suite of wireline geophysical well logs from four wells in a field onshore Niger Delta were examined and analyzed. Four hydrocarbon bearing reservoirs, which extended across all the wells were delineated. Stratigraphic correlation using lithology and resistivity logs reveal that the area of study is composed of alternating sands and shales.

Subsurface velocity distribution derived from sonic logs attest to the same phenomenon of sand-shale interbedding. The velocity range is from 2700m/s to 3900m/s and that of reflection coefficient from -0.174 to 0.152. Compaction trend graphs show that velocity increases with depth and areas where there, are deviations from the normal trend line mark over pressured zones. Computed petrophysical parameters from well logs, indicate that most of the reservoirs are prolific in terms of hydrocarbon production. Reservoir A has average porosity of 22%, permeability 979mD, hydrocarbon saturation 56% and net to gross sand thickness ratio of 0.85. Reservoir B has average porosity of 21%, permeability 1051mD, hydrocarbon saturation 79% and a net to gross sand thickness ratio of 0.96. Reservoir C has an average porosity of 22%, permeability 1140mD, hydrocarbon saturation 68%, and a net to gross sand thickness ratio of 0.81. Reservoir D has an average porosity of 21%, permeability 562 mD, hydrocarbon saturation 64% and net to gross sand thickness ratio of 0.77. The data would serve as a vital asset for oil field development programmes.

KEYWORDS: Stratigraphy, permeability, compaction, porosity and overpressure.

INTRODUCTION

Reservoir characterization involves the quantification, intergration, reduction and analysis of geological, petrophysical, seismic and engineering data (Tinker, 1996). In exploration and production business, data from these sources are utilized to generate a three dimensional model of the subsurface. The challenge is quantification and risk assessment and making accurate predictions of reservoir parameters so that reservoirs can be exploited with as few wells as possible (Riel, 2000). Some important reservoir model parameters to which geophysical measurements can contribute include: Rock type and porosity, fluid content and properties, pressures, fracture orientation, associated uncertainties and all of the above, not in map form, but spatially. This article discusses the principles involved in the use of geophysical well logs in the characterization of potential hydrocarbon reservoirs.

Regional Geologic Setting of Niger Delta

The Niger Delta is situated on the Gulf of Guinea on the west coast of Central Africa (Figure 1). The delta is one of the world's largest with the subaerial portion covering about 75000km^2 and extending more than 300km from apex to mouth (Evamy et al., 1978; Short and Stauble, 1967). The study location lies onshore Niger Delta (Figure 1). The basin developed at the intersection of Benue Trough and South Atlantic ocean (Figure. 2) where a triple junction (ridge-ridge-ridge) developed during separation of South American sub-continent from Africa in the Early Cretaceous (Stoneley, 1966, Whiteman, 1982). Structural features such as Benin and Calabar hinge lines (Figure 3) delimit the basin in the north-western and north-eastern parts (Murat, 1970). Basement tectonism actually facilitated subsequent deposition and accumulation of clastic sediments within the basin.

Three subsurface lithofacies (Figure 4) have been identified in the subsurface of the basin and which are known in the oil industry parlance as Akata, Agbada and Benin Formations (Short and Stauble 1967; Doust, 1989, Evamy et al, 1978; Doust and Omatsola, 1990). Basinal tectonisin is characterized by growth faults and rollover anticlines. Evamy et al; 1978 classified these faults into structure building, crestal (synthetic and antithetic), flank and counter regional types (Figure. 5). Rollover anticlines are intimately associated with growth faults. Weber and Daukoru, 1975 and Haack et al; 2000 grouped them into simple rollover, faulted anticline, collapsed crest, closure behind fault and structural-stratigraphic types.

METHODOLOGY

The suite of borehole logs provided for this study are gamma ray (GR), spontaneous potential (SP), deep induction (ILD), spherically focused (SFL), conductivity Induction (CILD), and sonic log. The logs were analyzed and interpreted to meet the objectives of the study.

Lithology of the sampled zones was interpreted from gamma ray and spontaneous potential logs. The sand-shale ratio determination was based on Schlumberger (1991) and Xiao and Suppe (1989). Deflections above 75% from shale base-line connote sand, while 0 to 25% deflections indicate shale and greater than 25% to less than 75% deflections indicate intermediate shaly-sand.

The correlation exercise commenced with the setting of the composite logs from various wells side by side and using a regular spacing while keeping a reference datum for aligning the wells (Dikkers, 1985). The correlations utilized concept of similarity in log responses (Scra, 1986). Similar curve patterns identified at each well were correlated from one well to the other across the entire study area to produce the correlation section.

Interval transit times derived from sonic logs were plotted as a function of depth and a line of best fit drawn through the points to generate compaction trend graphs (Hillis, 1992). These graphs aided the study of compaction and

M. A. Ayuk, Applied Geophysics Department, Federal University of Technology, Akure, Nigeria.
M. T. Olowokere, Applied Geophysics Department, Federal University of Technology, Akure, Nigeria.
E. A. Ariyibi, Department of Physics, Awolowo University, Ile-Ife, Nigeria

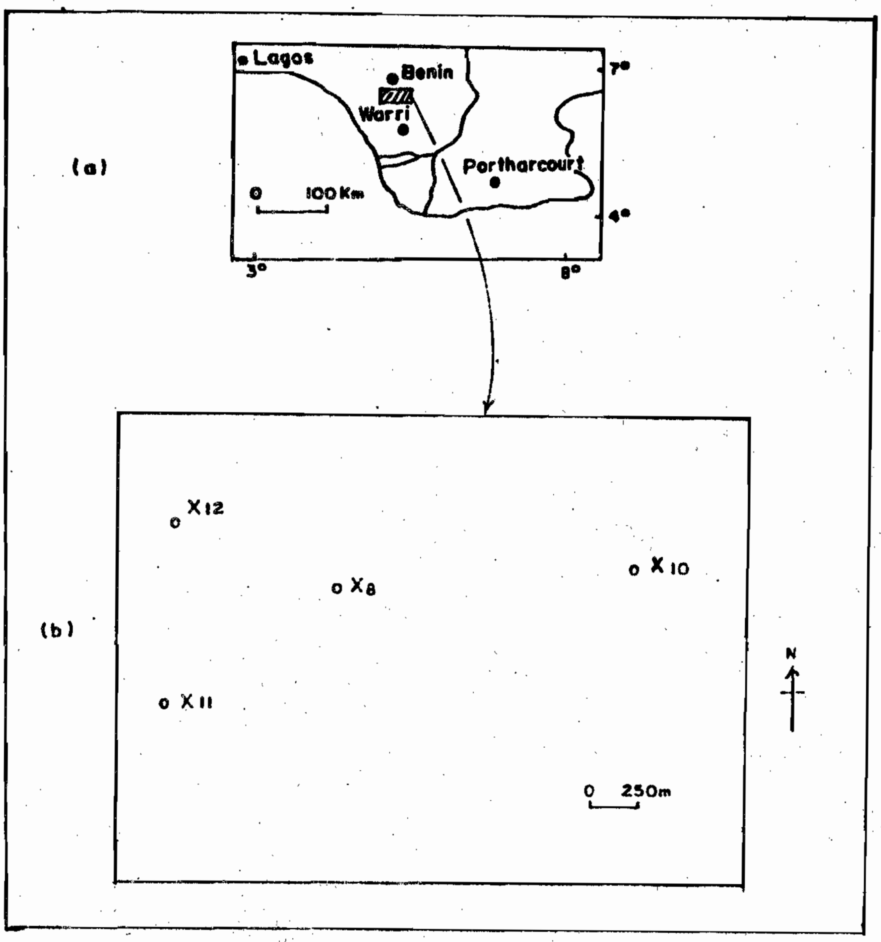

Fig. 1 (a) Index map of Niger Delta with study location (Evamy etal, 1978).
(b) Location map of study area.

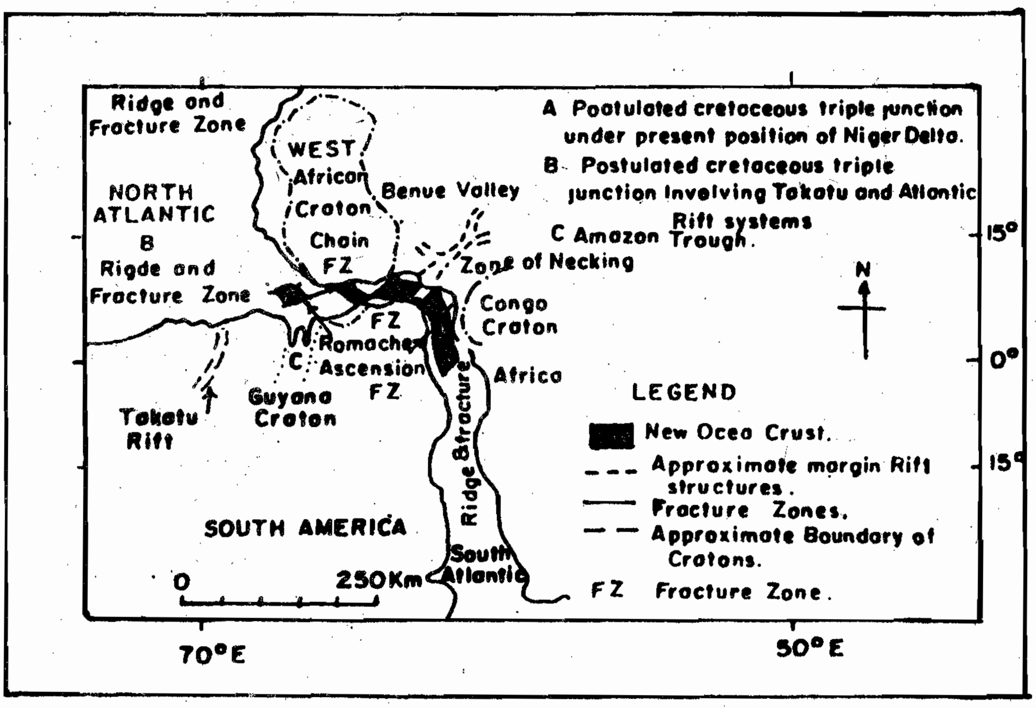

Fig. 2: Position of Niger Delta triple junction (Whiteman, 1982).

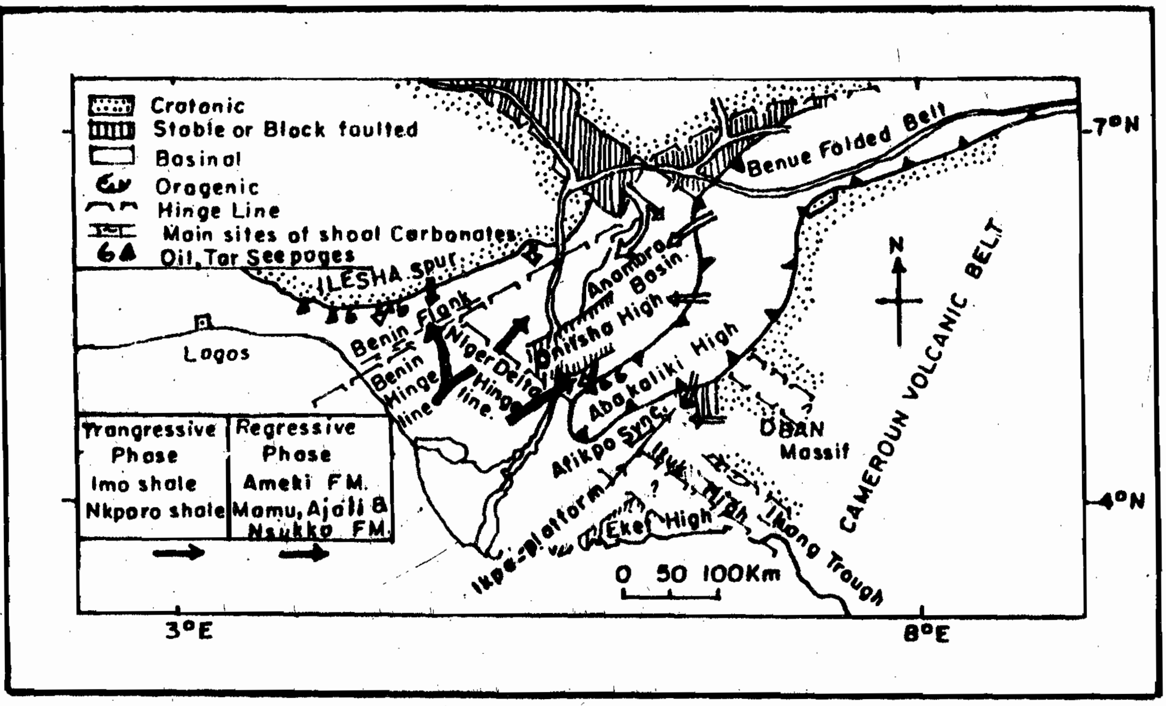

Fig. 3 : Lower Coniacian – Lower Eocene evolution of Niger Delta (Murat, 1970).

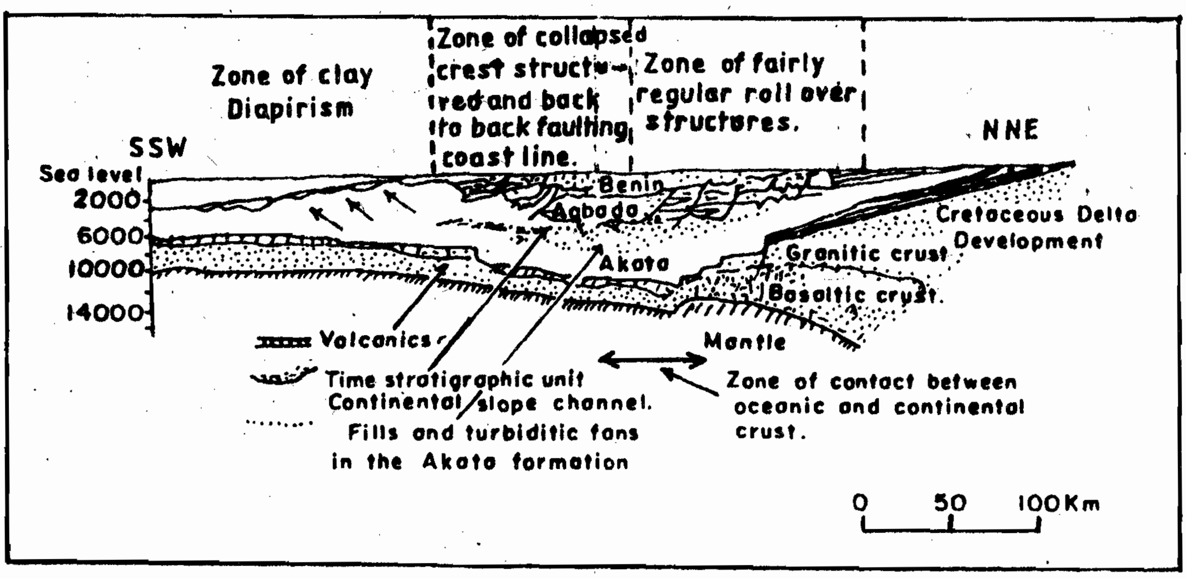

Fig. 4: Schematic dip section of the Niger Delta (Whiteman, 1982)

overpressure history of the study area, (Schlumberger, 1985). Reflectivity series for all the wells were produced from Gardner et al, (1974) empirical equation using interval velocities derived from sonic logs. The logs sampled at various depths along the wells were digitized and relevant petrophysical parameters computed.

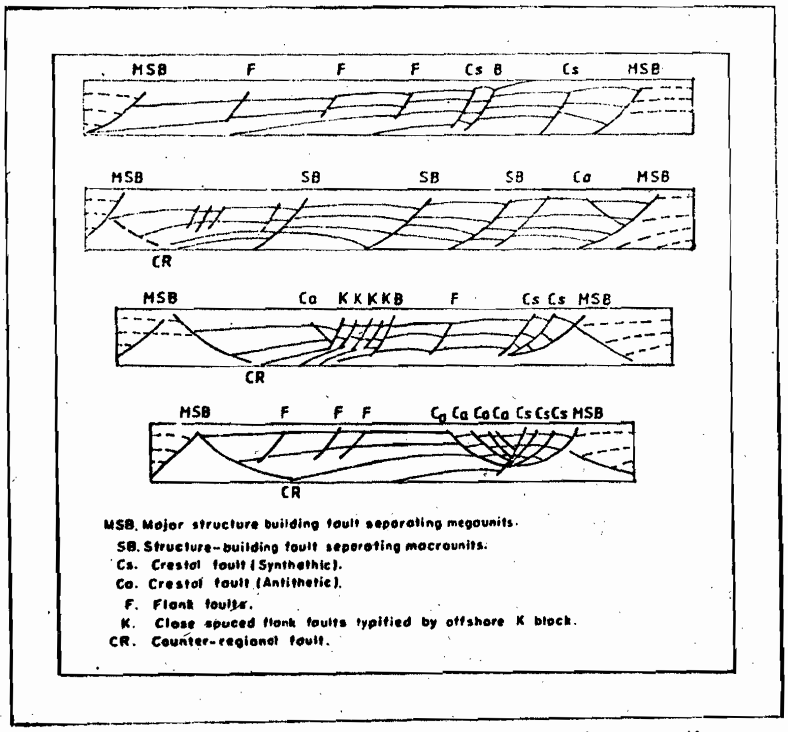

Fig. 5 : Classification of Synsedimentary faults and mega-units (Evamy et al; 1978).

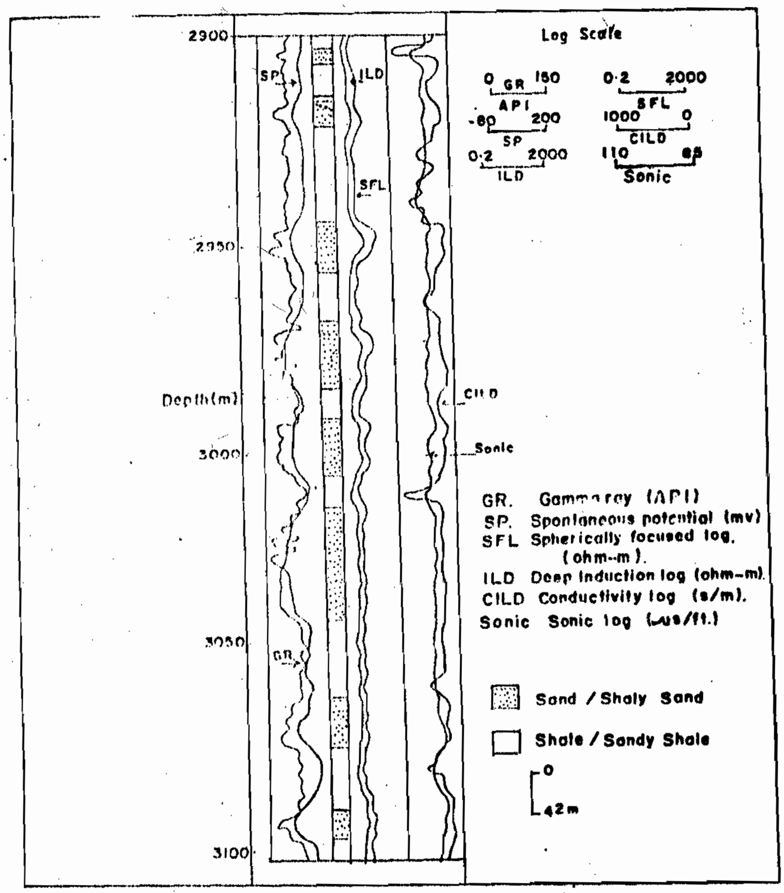

Fig. 6 : Composite well logs of well X12 and Lithology interpretation

DISCUSSION OF RESULTS

(a) Lilhology, Correlation Panel, Compaction Trend Graphs and Reflectivity Series

Figure 6 depicts the interpreted lithology. It is composed of alternating sand/shaly-sand and shale/sandy shale units. Lithologic correlation section that trend in northwest to southeast direction corroborates this fact and the section is sampled by four wells (figure 7). The sands which are generally dirty extend across all the wells. The shales which are interbedded within the sands have the same trend, but increases in thickness with depth. Four potential hydrocarbon reservoirs designated A, B, C and D were recognized (figure. 7). The reservoirs are stratified and occur at various depth. Their thicknesses along and across the holes vary, and they are all dirty. They have also suffered significant deformation and their shale content increases with depth along the wells.

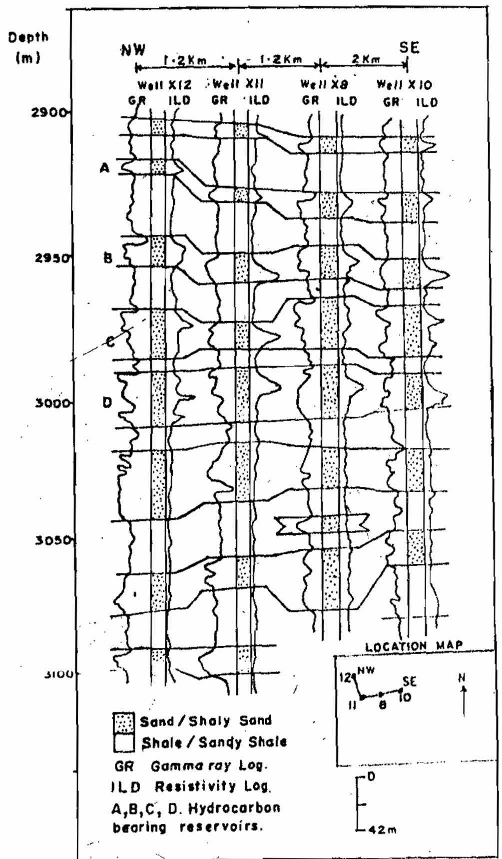

Fig. 7: Lithostratigraphic correlation panel with hydrocarbon bearing reservoirs.

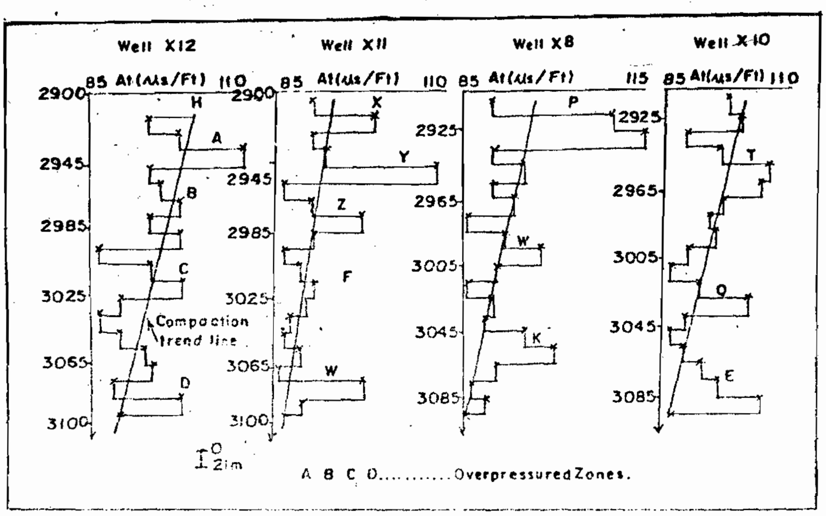

Fig. 8: Graphs showing compaction trend lines and overpressured zones in the study area.

It can be deduced from the graphs (Figure. 8) that compaction increases with depth. The oscillating nature of the interval transit time curves is an indication that this zone is of mixed compaction; characteristic of the interbedded sands and shales of the Agbada formation (Evans et al, 1975). The facies are also hydrostatically pressured and overpressured. Overpressured zones occur where there is prominent deviation to the right of compaction trend lines. The zones in most cases correspond to caprock or seals to potential reservoirs, and only in few cases do we have exception from this trend.

Reflectivity series graphs (Figures 9a and b) along the wells indicate that reflection coefficient is irregularly distributed. This parameter portrays rock interfaces typical of sand-shale interbedding. Interval velocities vary both laterally and vertically in the study area.

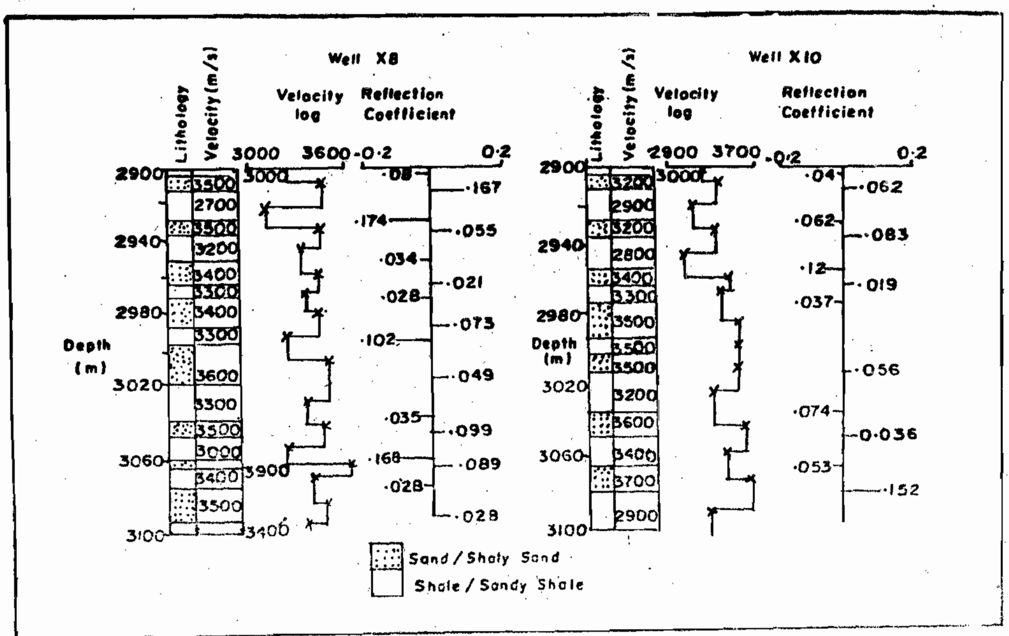

Fig. 9a: Lithology, interval velocities and reflectivity series of wells 8 and 10.

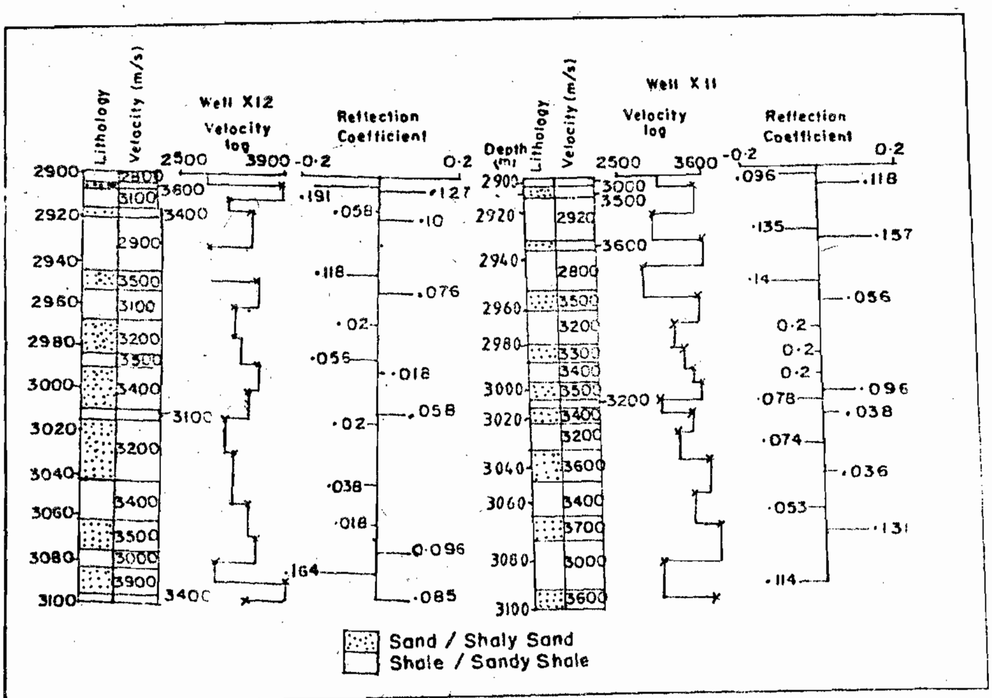

Fig. 9b: Lithology, interval velocities and reflectivity series of wells 11 and 12.

(b) Petrophysics of Potential Hydrocarbon Reservoirs

Important petrophysical parameters for all the hydrocarbon bearing reservoirs have been computed and displayed in Table 1. The reservoirs (Figure. 7) are labeled A, B, C and D, respectively.

RESERVOIR A

This reservoir occurs at an average depth of 2928m. The depth range across the wells is from 2918 to 2933m, implying significant deformation. It has an average gross sand thickness of 5m, net sand thickness, 4m and net to gross sand

Table 1: Reservoir model parameters derived from geophysical wireline logs.

a. Reservoirs depth (m)

Reservoirs	Well 12	Well 11	Well 8	Well 10	Average
A	2918	2929	2933	2933	2928
B	2948	2955	2958	2960	2955
C	2974	2980	2979	2984	2979
D	2997	2995	2994	2998	2996

b. Gross sand Thickness (m)

Reservoirs	Well 12	Well 11	Well 8	Well 10	Average
A	3.0	2.5	7.5	8.0	5.5
B	9.0	9.5	13.0	8.0	9.9
C	18.0	7.5	16.0	21.0	15.6
D	18.0	8.5	22.0	11.0	14.9
Total	48.0	28.0	58.5	48.0	

c. Net sand thickness (m)

Reservoirs	Well 12	Well 11	Well 8	Well 10	Average
A	3.0	2.5	7.5	8.0	4.0
B	9.0	9.5	12.0	7.3	9.5
C	16.0	6.1	11.3	17.0	12.6
D	14.0	5.5	16.0	10.0	11.4
Total	42.0	23.6	46.8	37.3	

d. Net to gross sand thickness (%)

Reservoirs	Well 12	Well 11	Well 8	Well 10	Average
A	100	100	100	38	85
B	100	100	92	91	96
C	89	81	71	81	80.5
D	78	65	73	91	76.8

e. Volume of shale V_{sh}(%)

Reservoirs	Well 12	Well 11	Well 8	Well 10	Average
A	13.2	10.8	4.0	25.6	13.4
B	13.2	6.8	28.5	6.9	13.9
C	10.5	26.9	11.1	12.7	15.3
D	10.5	20.6	36.8	21.8	22.4
Average	11.9	16.3	20.1	16.8	

f. Porosity ($\emptyset_e$)%

Reservoirs	Well 12	Well 11	Well 8	Well 10	Average
A	22.7	20.7	23.1	19.3	21.5
B	21.7	21.1	17.4	24.6	21.2
C	24.2	20.7	22.0	21.0	22.0
D	23.3	19.0	14.0	17.5	20.9
Average	23.0	20.4	19.1	20.1	

g. Resistivity index (I)

Reservoirs	Well 12	Well 11	Well 8	Well 10	Average
A	10	1.0	27	6.0	11
B	30	17	30	20	24
C	25	5.0	10	10	13
D	13	6.0	10	6.0	9.0
Average	20	7.0	19	11	

h. Hydrocarbon saturation (S_h)%

Reservoirs	Well 12	Well 11	Well 8	Well 10	Average
A	68.	13.4	80.6	60.0	55.6
B	81.7	75.5	81.7	77.6	79.1
C	80.0	55.3	67.7	68.4	67.9
D	71.7	59.2	68.4	55.3	63.7
Total	75.5	50.9	74.6	65.3	

i. Irreducible water saturation (S_{wi})%

Reservoirs	Well 12	Well 11	Well 8	Well 10	Average
A	9.9	10.8	9.7	11.6	10.5
B	10.3	10.6	10.9	10.6	10.4
C	9.2	10.8	12.9	9.1	10.1
D	9.6	11.8	16.0	12.8	12.6
Average	9.8	11.0	12.4	11.0	

j. Permeability K (mD)

Reservoirs	Well 12	Well 11	Well 8	Well 10	Average
A	1291	716	1454	453	978.5
B	974	810	230	2193	1051.2
C	1993	716	1056	793	1139.5
D	1544	40.8	56	239	561.8
Average	1451	571	691	920	

k. Relative permeability to oil K_{10}(%)

Reservoirs	Well 12	Well 11	Well 8	Well 10	Average
A	56.1	1.9	78.8	44.3	45.3
B	82.2	70.1	87.4	71.6	77.8
C	76.6	36.6	55.3	57.0	56.4
D	61.5	43.3	65.0	38.4	52.1
Average	69.1	38.0	71.6	52.8	

l. Interval velocity (m/s)

Reservoirs	Well 12	Well 11	Well 8	Well 10	Average
A	3400	3600	3500	3200	3425
B	3500	3500	3400	3400	3450
C	3200	3300	3400	3500	3350
D	3400	3500	3600	3500	3500
Average	3400	3500	3500	3400	